Journal of Inflammation Research

Dovepress
Taylor & Francis Group

Open Access Full Text Article

ORIGINAL RESEARCH

Swainsonine Protects Human Thyrocytes from Fas-Induced Apoptosis: In vitro Study on Nthy-Ori 3-1 Cell Line

Sara Trzos[1,2], Małgorzata Opydo[3], Michał Bochenek[4], Paweł Link-Lenczowski[5,6], Ewa Pocheć[1]

[1]Department of Glycoconjugate Biochemistry, Institute of Zoology and Biomedical Research, Faculty of Biology, Jagiellonian University, Krakow, Poland; [2]Doctoral School of Exact and Natural Sciences, Jagiellonian University, Krakow, Poland; [3]Laboratory of Experimental Hematology, Institute of Zoology and Biomedical Research, Faculty of Biology, Jagiellonian University, Krakow, Poland; [4]Flow Cytometry Facility, Institute of Zoology and Biomedical Research, Malopolska Centre of Biotechnology, Jagiellonian University, Krakow, Poland; [5]Department of Medical Physiology, Institute of Physiotherapy, Jagiellonian University Medical College, Krakow, Poland; [6]Center for the Development of Therapies for Civilization and Age-Related Diseases, Jagiellonian University Medical College, Krakow, Poland

Correspondence: Ewa Pocheć, Department of Glycoconjugate Biochemistry, Institute of Zoology and Biomedical Research, Faculty of Biology, Jagiellonian University, Gronostajowa 9, Krakow, 30-387, Poland, Tel +48 12 664 64 67, Email ewa.pochec@uj.edu.pl

Background: The role of Fas is crucial for preserving immunotolerance. The mechanisms and roles of Fas/FasL signaling in the immune system are well understood, but the knowledge of how this process is regulated remains limited. Fas-mediated apoptosis is a way of thyrocyte elimination and thyroid destruction in Hashimoto's thyroiditis (HT). Proinflammatory cytokines, produced abundantly by immune cells in the thyroid in HT, stimulate the expression of Fas in thyrocytes, making them susceptible to apoptosis induced by FasL on the immune cell surface.

Purpose: The present study aimed to evaluate the impact of changes in Fas *N*-glycosylation on the death of human follicular thyroid cells of the Nthy-ori 3–1 line.

Methods: To induce thyrocyte apoptosis, an in vitro model was established. Cells were stimulated with IFNγ to express Fas and treated with the *N*-glycosylation inhibitors, kifunensine and swainsonine. Then apoptosis was induced by human recombinant FasL. MALDI-Tof mass spectrometry monitored kifunensine- and swainsonine-induced changes in *N*-glycosylation of Nthy-ori 3–1 thyrocytes, and cell death was analyzed using flow cytometry (annexin V staining, caspase 3/7 activity, TMRE mitochondrial membrane potential assay) and fluorescence microscopy (DAPI staining).

Results: We found that swainsonine reduces Nthy-ori 3–1 cell apoptosis, caspase 3 and 7 activity, and restores mitochondrial potential. DAPI staining showed a decreased rupture and fragmentation of Nthy-ori 3–1 cell nuclei in the presence of swainsonine. The protective effect of kifunensine was only shown in the TMRE assay and for the late apoptotic cells in annexin V^+/PI^+ staining.

Conclusion: Our study demonstrated for the first time the anti-apoptotic effect of swainsonine on follicular thyroid cell death through the Fas/FasL signaling pathway. This finding may have later applications in controlling Fas/FasL-induced thyrocyte apoptosis and preventing thyroid destruction in HT.

Keywords: apoptosis, Fas/FasL pathway, glycosylation, kifunensine, swainsonine, thyrocyte

Introduction

Apoptosis is a form of cell death fundamental to the normal development of an organism. It allows the body to maintain homeostasis and tissue remodeling.[1–3] It participates in T and B cell death to limit excessive immune responses.[4] To prevent damage to normal cells, immune cells targeting their antigens undergo apoptosis. However, disruption of apoptosis can have serious consequences for the body, leading to autoimmunity.[1,4]

During apoptosis, characteristic changes in cell morphology occur. In the first stage, cell shrinkage and chromatin condensation (pyknosis) can be observed. This is followed by the fragmentation of a nucleus (karyorexia) and the

Received: 14 April 2025
Accepted: 7 August 2025
Published: 14 September 2025

Graphical Abstract

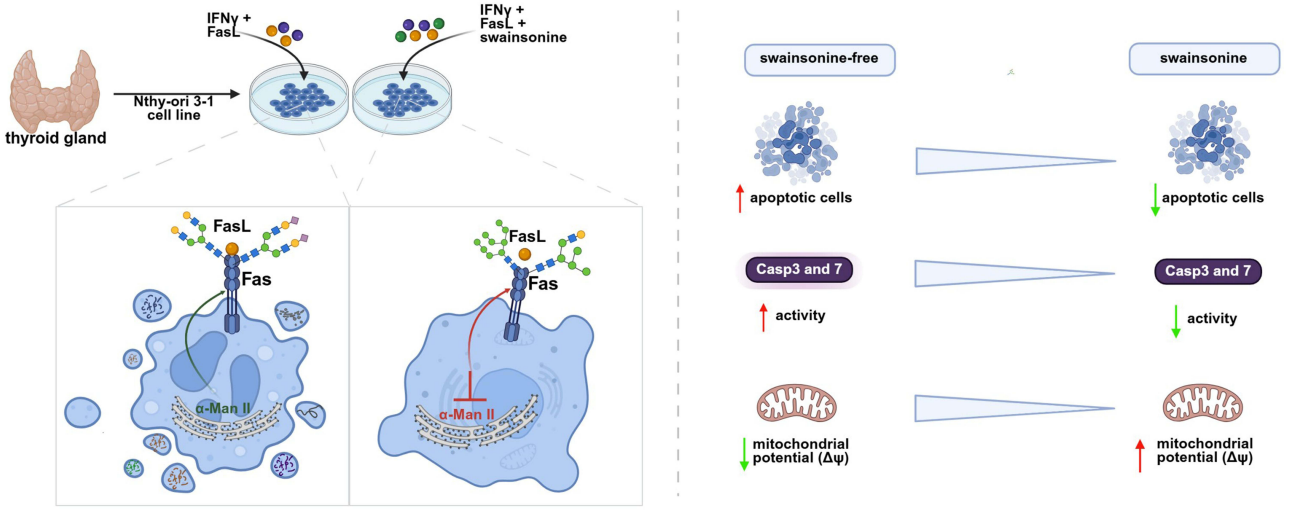

formation of apoptotic bodies, which contain cytoplasm, organelles, and fragments of the cell nucleus. Eventually, the apoptotic bodies are phagocytosed by macrophages and degraded in phagolysosomes.[2,5]

In the process of apoptosis, two pathways are distinguished: intrinsic and extrinsic, which are interrelated. The Fas/FasL system is the most extensively studied extrinsic apoptosis pathway. FasL (CD95) in its trimer form binds and attaches to Fas, inducing its trimerization. Fas then binds to the Fas-associated death domain (FADD), to which caspase (Casp) 8 attaches.[4] Casp 8, FADD, and the death receptor form a death-inducing signaling complex (DISC), which activates Casp 8. Consequently, Casp 8 undergoes the conformational change necessary for its enzymatic activity. In addition, Casp 8 undergoes autoproteolytic processing and detaches itself from the DISC, gaining access to substrates in other parts of the cell. Upon activation, Casp 8 cleaves procaspases 3, 6, and 7 through proteolytic cutting and produces effector caspases. Casp 8 can also cleave the proapoptotic protein Bid to tBid, which initiates the intrinsic apoptotic pathway and promotes mitochondrial outer membrane permeabilization (MOMP) and cytochrome c release.[4,6] Activation of both pathways ultimately leads to cell death.[1,7,8]

Apoptosis activated by the Fas molecule also results from the disappearance of immunotolerance that is inherent in autoimmunity, including the development of Hashimoto's thyroiditis (HT). Under physiological conditions, Fas is present on the surface of thyrocytes in an inactive state. Activation of death receptors occurs under the influence of pro-inflammatory cytokines that are produced by $CD4^+$ T lymphocytes, and the interaction of Fas protein with its receptor (FasL) present on the surface of immune cells activates thyroid cell death.[9,10] An increase of Fas expression on thyrocytes has been demonstrated in HT patients compared to healthy subjects, therefore, the Fas/FasL signaling pathway is considered a major mechanism of T-cell-mediated thyrocyte apoptosis.[1,10,11]

Glycosylation is the enzymatic attachment of glycans to proteins.[11] Protein *N*-glycosylation involves the formation of an *N*-glycosidic bond between *N*-acetylglucosamine (GlcNAc) and the nitrogen atom in the amide group of asparagine (Asn). The formation of the mature *N*-oligosaccharide structures occurs in several steps in the rough endoplasmic reticulum (RER) and Golgi apparatus (GA), and requires the activity of several enzymes from the glycosidase and glycosyltransferase families.[12–14]

N-glycosylation of Fas regulates the activity of the protein by modifying its interaction with a ligand (FasL) or forming signaling complexes. *N*-oligosaccharide attachment sites are located in the extracellular domain at positions N118 and N136, close to the FasL binding site, and it seems possible that *N*-glycosylation affects the Fas-FasL interaction and thus the apoptosis pathway.[11,15,16] It has been shown that *N*-glycosylation is not essential for Fas to bind to FasL but modulates this interaction. Enzymatic removal of sugar structures from the Fas molecule partially

inhibits recruitment of FADD to DISC but slows activation of procaspase 8 in DISC.[16,17] In HD3 colon cancer cells, silencing of sialyltransferase 1 (ST6Gal I), which catalyzes the attachment of α2,6-sialic acid (SA) to *N*-oligosaccharides, showed that SA reduces receptor oligomerization and FasL-induced signaling. An increase in SA α2,6-linkage results in inhibition of Fas ligand binding to FADD and prevents further signaling associated with regulatory cell death. The control of receptor conformation and the development of a functional trimer appears to be a mechanism of apoptosis dependent on the sialylation of the Fas molecule.[18]

Understanding cell death regulation, among other changes in glycosylation of death receptors, is important to finding treatments for hyper-reactive immune responses.[18] Glycosylation inhibitors such as kifunensine (Kf) and swainsonine (Sw) are useful tools for rearrangement glycosylation. Kf, an alkaloid isolated from the bacterium *Kitasatosporia kifunense*, inhibits α-mannosidase I in RER, thus blocking the formation of hybrid- and complex-type *N*-oligosaccharides (Figure 1A). Sw is a plant alkaloid from *Swainsonona canescens* that inhibits α-mannosidase II in GA and prevents the remodeling of hybrid- to complex-structures (Figure 1B).[19] The study showed that Sw treatment induced apoptosis of esophageal squamous cell carcinoma (Eca-109 cell line) in vitro. An increase in the expression of the proapoptotic protein BAX was observed, which correlated with a decrease in the expression of the antiapoptotic molecule BCL-2. Sw administration also induced translocation of BAX into mitochondria, destruction of their integrity, resulting in the subsequent release of cytochrome c, which in turn activated Casp 9 and 3.[11,20]

Our study aimed to assess if *N*-glycosylation of thyrocytes affects their apoptosis via the Fas-FasL signaling pathway in an in vitro model of Hashimoto's thyroiditis. Two potent glycosylation inhibitors, with precise mechanisms of action, Kf, and Sw, were used to modify the *N*-glycosylation of human thyrocytes of the Nthy-ori 3–1 cell line. The cells were stimulated with interferon-gamma (IFNγ), a proinflammatory cytokine, to activate Fas expression, and incubated with glycosylation inhibitors to block the glycosylation at the stage of oligomannose structures (Kf) or oligomannose/hybrid-type *N*-glycans (Sw), preventing the synthesis of complex-type structures identified on Fas protein. Fas signaling resulting in thyrocyte apoptosis was then activated with human recombinant FasL. The glycomic approach used in the study, MALDI-ToF (matrix-assisted laser desorption/ionization with time-of-flight analyzer) mass spectrometry, together with the state-of-the-art linkage-specific sialic acid derivatization of *N*-glycans, enabled us to precisely track the changes in the glycomes of treated Nthy-ori 3–1 thyrocytes. Apoptosis was detected by flow cytometry (annexin V assay, Casp 3/7 activity, and mitochondrial potential) and fluorescence microscopy evaluation of cell nuclei stained with DAPI. This

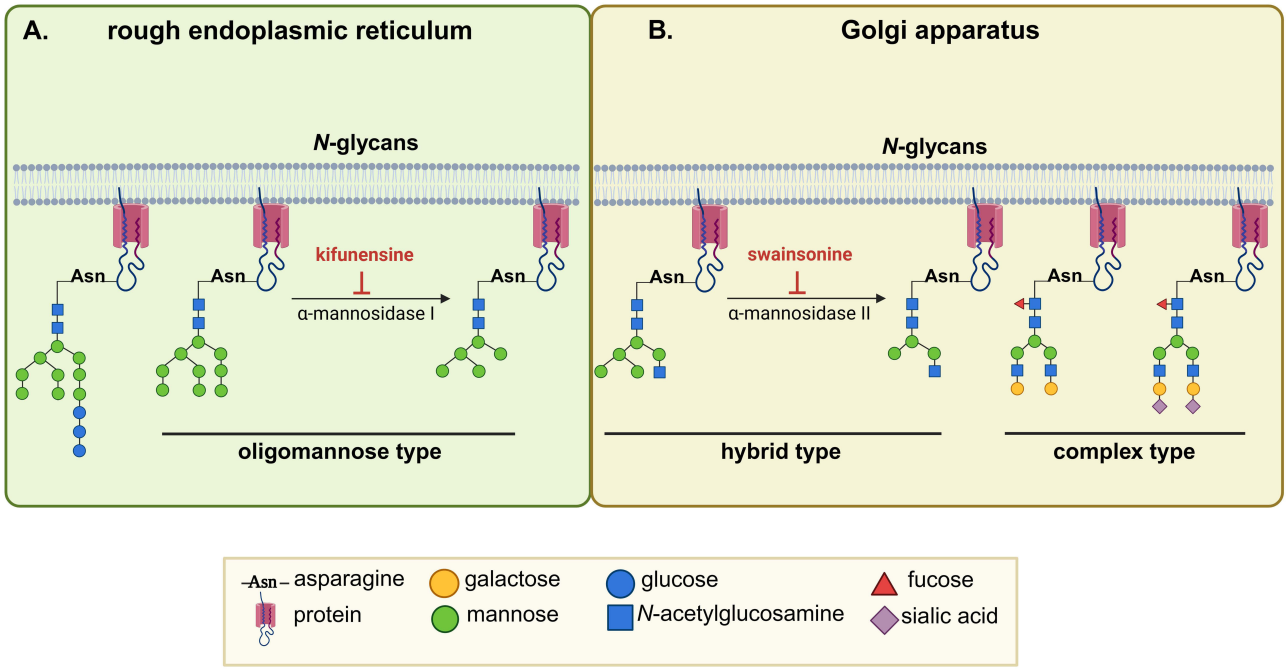

Figure 1 Scheme of kifunensine (**A**) and swainsonine (**B**) action. Created in BioRender. Trzos, S. (2025) https://BioRender.com/1xruw6b.

https://doi.org/10.2147/JIR.S529858

combination of glycomic studies and the essential aspects of the biology of cell death allowed us to analyze human thyrocyte biology in a way that has not been studied before. Significant reduction of Fas-mediated apoptosis in swainsonine-treated thyrocytes, as shown by the assays detecting apoptotic changes at different stages of this process, led us to the conclusion that complex-type *N*-glycans are crucial to fully efficient apoptosis of thyroid follicular cells. To the best of our knowledge, our results are the first which show that swainsonine may act as an inhibitor of thyrocyte apoptosis.

Materials and Methods

In vitro Culture and Stimulation of Human Thyroid Follicular Epithelial Cells

Human thyroid follicular epithelial cells (thyrocytes) of the Nthy-ori 3–1 cell line (ECACC, RRID: CVCL 2659), obtained from the Department of Biochemistry and Molecular Biology at the Medical Center for Postgraduate Education in Warsaw (Poland), courtesy of Professor Barbara Czarnocka, were used in the study. Nthy-ori 3–1 cells were harvested from a 35-year-old woman and immortalized with a plasmid containing the SV40 virus genome. It is the only normal human thyroid cell line to exhibit thyroid-specific functions such as thyroglobulin production and iodine uptake.[21,22] The study was registered by the Ministry of Climate and Environment (01.2–96/2022) due to the classification of the cell line as a Genetically Modified Organism Class 1 (GMO1).

Human thyrocytes were cultured in RPMI 1640 medium (72400, Gibco, Paisley, UK) supplemented with 10% fetal bovine serum (FBS, 10270, Gibco, Paisley, UK), 100 U/mL penicillin, and 100 µg/mL streptomycin (15140, Gibco, Paisley, UK). Cells were cultured under 2D conditions in normoxia (5% CO_2 and 21% O_2) at 37°C in an incubator (Forma Steri-Cycle i160, Thermo Fisher Scientific, Rockford, IL, USA). Cell passages were performed after reaching approximately 80% confluence. Thyrocytes were used for experiments at low passages after recovery from the bank. A MycoAlertTM plate kit (LT07-418, Lonza, Basel, Switzerland) was used to check whether cells were contaminated with *Mycoplasma* sp.[23]

To activate Fas-FasL signaling in an in vitro model and assay the effect of glycosylation inhibitors on thyrocyte apoptosis, the Nthy-ori 3–1 cell line was spread into 12-well plates (for flow cytometry) or 4-well plates (for fluorescence microscopy) at a density of 2×10^4 cells/well, and into 60 mm dishes (for MALDI-Tof MS and SDS-PAGE) at a density of 5×10^5 cells/dish. The next day cells were stimulated with the recombinant human IFNγ (300–02, PeproTech, London, UK) in the concentration of 20 ng/mL, based on the previous study by Wang et al.[23] To modify glycosylation 5 µM kifunensine (10009437, Cayman Chemical, Ann Arbor, MI, USA), and 2.5 µg/mL swainsonine (16860, Cayman Chemical, Ann Arbor, MI, USA) were added to the appropriate wells and dishes. The incubation with IFNγ and the glycosylation inhibitors was carried out for 72 h. On the fourth day of the experiment, recombinant human FasL (ab157085, Abcam, Boston, MA, USA) was added to the wells/dishes at a concentration of 20 ng/mL, selected based on the study by Cui et al.[24] Incubation was carried out for 16 hours until cells were harvested for experiments. In addition to the experimental variants (IFNγ+FasL, IFNγ+FasL+Kf, IFNγ+FasL+Sw), several controls (untreated cells, Kf, Sw, IFNγ, IFNγ+Kf, IFNγ+Sw) were prepared. The stimulation scheme of Nthy-ori 3–1 cells is shown in Figure 2.

Fas Protein Expression

To determine if IFNγ (20 ng/mL) and the glycosylation inhibitors: swainsonine (2.5 µg/mL) and kifunensine (5 µM) affect Fas protein expression, a flow cytometry method was used according to manufacturer's recommendations. Cells were stimulated as shown in Figure 2. Nthy-ori 3–1 cells were harvested by 0.25% trypsin-EDTA (25200056, Gibco, Paisley, UK) and spun at 1100 rpm for 5 min. The cell pellets were resuspended in 50 µL warm PBS, and 0.75 µL of phycoerythrin (PE)-conjugated anti-Fas antibody (130–113-069, Miltenyi Biotec, Bergisch Gladbach, Germany) was added. PE-labeled recombinant human IgG1 (130–113-438, Miltenyi Biotec, Bergisch Gladbach, Germany) was used as an isotype control. Samples were kept for 35 minutes on ice in the dark. To identify necrotic cells, 0.5 µL of propidium iodide (PI; 556547, BD Biosciences, San Diego, CA, USA) was added. Incubation was carried out for 5 min under the same conditions. Labeled cells were resuspended in 400 µL of PBS and analyzed. For analysis using a Navios flow

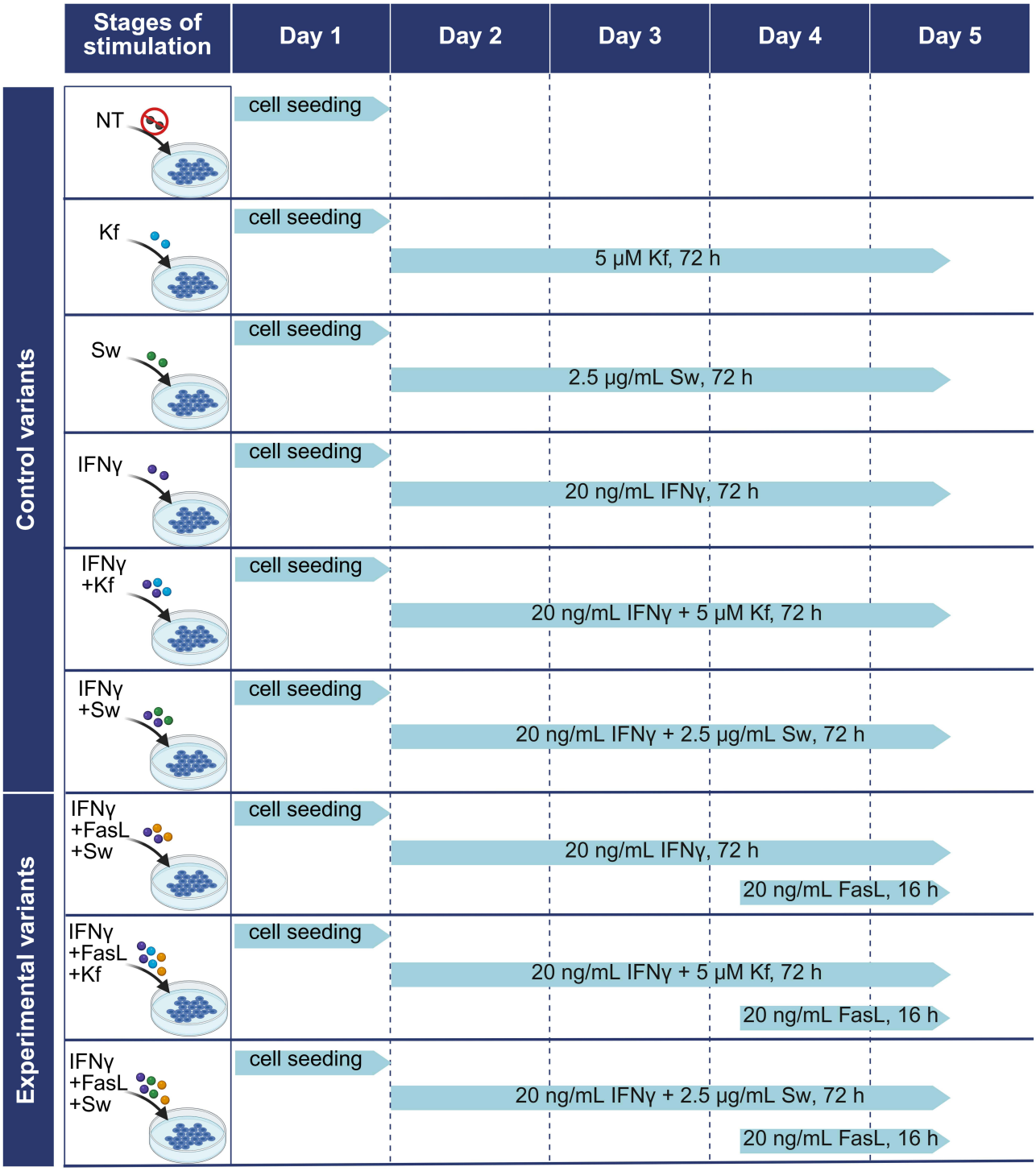

Figure 2 Treatment regimen for Nthy-ori 3–1 cells in an in vitro model to induce apoptosis. Created in BioRender. Trzos, S. (2025) https://BioRender.com/7vei5yk.
Abbreviations: FasL, Fas ligand; IFNγ, interferon-gamma; Kf, kifunensine; Sw, swainsonine.

cytometer (Beckman Coulter, Bread, CA, USA), 1×10^4 cells/sample were used. Evaluation of Fas protein expression on the surface of thyrocytes was performed using Kaluza Analysis 2.2.1 software (Beckman Coulter, Bread, CA, USA).

alamarBlue Assay

The alamarBlue assay was used to assess the viability of Nthy-ori 3–1 cells according to the manufacturer's protocol. Briefly, cells were passaged into 96-well black plates with clear bottoms at a density of 1×10^4 cells per well. On the

https://doi.org/10.2147/JIR.S529858

following day, glycosylation inhibitors were added at a concentration range of 1–100 μM for Kf and 1–100 μg/mL for Sw. Incubation was carried out for 24, 48, and 72 hours. After the specified incubation times, alamarBlue reagent (DAL1025, Thermo Fisher Scientific, Rockford, IL, USA), which had been previously diluted in PBS (14190, Gibco, Paisley, UK) at a ratio of 1:10, was added to each well. Cells were incubated for 2 hours. Fluorescence intensity was measured for an excitation wavelength of 560 nm and an emission wavelength of 595 nm in an Infinite F200 Pro reader (Tecan, Männedorf, Switzerland). Cell viability was determined as a percentage of the value of cells untreated with inhibitors.

Cell Lysis and Determination of Protein Concentration

Total homogenates from the cells were obtained in a radioimmunoprecipitation buffer (RIPA; 89900, Thermo Fisher Scientific, Waltham, MA, USA) containing a protease inhibitor mix (P8340, Sigma-Aldrich, Saint Louis, MO, USA). Protein concentration was determined using the Micro BCA™ Protein Assay Kit (23235, Thermo Fisher Scientific, Waltham, MA, USA). Twenty μg of protein was reversed in SDS-PAGE, and 100 μg of protein was subjected to glycosylation analysis using MALDI-Tof mass spectrometry.

CBB Staining and Lectin Blotting

CBB staining and lectin blotting were prepared as described previously.[25] Extracted proteins were separated by SDS-PAGE under reducing conditions. For analysis of protein profiles, gels were stained using Coomassie brilliant blue (B-2025, Sigma, Saint Louis, MO, USA). In addition to identifying differences in the *N*-oligosaccharide pool in the presence of Kf and Sw, protein electrotransfer was performed onto a polyvinylidene fluoride membrane (PVDF, 88518, Thermo Fisher Scientific, Waltham, MA, USA). Target sugar structures were detected using lectins of selected specificity: *Galanthus nivalis* lectin (GNL) (B-1245, Vector Laboratories, Newark, CA, USA) recognizing oligomannose *N*-glycans, and *Phaseolus vulgaris* lectin (PHA-L) (B-1115, Vector Laboratories, Newark, CA, USA) binding three- and four-antennary complex-type structures, followed by alkaline phosphatase-conjugated extravidin (E2636, Sigma-Aldrich, Saint Louis, MO, USA). Glycoproteins were colorimetrically visualized using a substrate consisting of nitrotetrazolium blue chloride (NBT; 11383213001, Roche Diagnostics GmbH, Basel, Switzerland), and 5-bromo-4-chloro-3-indolyl-phosphate, 4-toluidine salt (BCIP; 11383221001, Roche Diagnostics GmbH, Basel, Switzerland).

MALDI-Tof MS

Protein Precipitation and Enzymatic Digestion of *N*-Glycans

Before the *N*-glycan digestion procedure, 100 μg of protein was chemically precipitated from cell lysates using methanol and chloroform according to the previously published protocol.[26] To the precipitated protein, 20 μL of denaturing buffer (B1704S, New England Biolabs, Ipswich, MA) was added and incubated at 60°C for 10 minutes. In the next step, 31 μL of a solution consisting of Glycobuffer 2 (B3704S, New England Biolabs, Ipswich, MA), 10% NP-40 (B2704S, New England Biolabs, Ipswich, MA) and PNGase F (500,000 U/mL, P0705L, New England Biolabs, Ipswich, MA) was added to the samples. Samples were incubated overnight at 37°C. The released *N*-oligosaccharides were desalted on Supelclean™ ENVI-Carb™ SPE columns (57109-U, Sigma-Aldrich, St. Louis, MO, USA) according to the procedure described previously.[27] Finally, the *N*-glycans were concentrated in a lyophilizer (Labconco) under conditions: 0.051 mBar, −50°C overnight.

Derivatization of Sialic Acid

Derivatization of SA was performed according to the protocol.[28] Briefly, 1 μL of Milli-Q and 20 μL of a reaction mix consisting of 0.25 M 1,ethyl-3-(3-(dimethylamino)propyl)carbodiimide hydrochloride (EDC; PA-03-0849-P, Pol-aura, Zawroty, Poland), 0.25 M 1-hydroxybenzotriazole (HOBt; A0403978, Acros organics, Geel, Belgium) in ethanol (603-002-00-5, Stanlab, Lublin, Poland) were added to *N*-oligosaccharides samples, and incubated (1 hour, 37°C). The derivatization reaction was inhibited with 20 μL of acetonitrile (CHS-1201.2500, Chemsolve, Lodz, Poland). Subsequently, *N*-glycans were enriched by cotton-HILIC SPE using in-house prepared microtips according to Reiding et al.[28] Glycans eluted in 10 μL Milli-Q were dried by vacuum centrifuge (SpeedVac Plus, Savant). Samples were

suspended in 2 µL of 5 mg/mL super-DHB (50862, Merck, Darmstadt, Germany) dissolved in 50% ACN with 1 mM NaOH. The samples with *N*-glycans were transferred to an MTP plate, AnchorChip 384BC (8280790, Brucker Daltonics, Bremen, Germany), and left for a few minutes to dry.

MALDI-Tof MS Analysis

N-glycan profile analysis was performed on a rapiFlex™ mass spectrometer (Bruker Daltonics, Bremen, Germany) and FlexControl software (Bruker Daltonics, Bremen, Germany). MALDI-ToF MS was calibrated with Peptide Calibration Standard II in the mass range of 700–3200 Da (Brucker, Daltonics, Bremen, Germany, 8222570). Mass spectra were analyzed in positive ion mode $[M+Na]^+$ in the *m/z* range from 1000 to 5000, with a total of 32000 laser shots per sample. *N*-glycan peaks, as well as their structures, were determined from *m/z* values using GlycoWorkbench software (version 2.0, European Carbohydrates DataBase project; http://www.eurocarbdb.org/). Quantitative analysis of the content of sugar structures was performed based on the relative intensity of *N*-glycan peaks, expressed as a percentage (%) of the total area of all peaks in the mass spectra.

Apoptosis Assays

Annexin V and Propidium Iodide Assay

Annexin V-FITC Apoptosis Detection Kit I (556547, BD Biosciences, San Diego, California, USA) was used to assess the percentage of apoptotic and necrotic cells. Nthy-ori 3–1 cells were harvested by 0.25% trypsin-EDTA (25200056, Gibco, Paisley, UK). Cells were washed with cold PBS while centrifuging at 1100 rpm, 5 min, 4°C. Then, 100 µL of binding buffer, 2.5 µL of annexin V, and 2.5 µL of propidium iodide (PI) were added to the cell suspension. Samples were incubated at room temperature (RT) in the dark. After 15 min, 400 µL of binding buffer was added and incubated on ice in the dark until measurement. For analysis using a Navios flow cytometer (Beckman Coulter, Bread, CA, USA), 1×10^4 cells/sample was used. The assessment of thyrocyte apoptosis/necrosis was performed using Kaluza Analysis 2.2.1 software (Beckman Coulter, Bread, CA, USA).

Caspase 3 and 7 Activity Assay

The CellEvent™ Caspase 3/7 Green Flow Cytometry Detection Kit (C10740, Invitrogen, Thermo Fisher Scientific, Waltham, MA, USA) was used to determine the activity of caspases 3 and 7.[29] Nthy-ori 3–1 cells were harvested by trypsinization and suspended in 0.5 mL of warm PBS. Next, the cells were labeled with 0.5 µL of CellEvent® Caspase-3/7 Green Detection Reagent and incubated (37°C, in the dark). After 25 min, 0.5 µL of 1 mM SYTOX AADvanced solution was added to the samples and incubated again for 5 min at 37°C. For analysis using a Navios flow cytometer (Beckman Coulter, Bread, CA, USA), 1×10^4 cells/sample was used. The assessment of caspase 3 and 7 activity was performed using Kaluza Analysis 2.2.1 software (Beckman Coulter, Bread, CA, USA).

Mitochondrial Membrane Potential Assay

The tetramethylrhodamine ethyl ester perchlorate (TMRE; 87917, Sigma-Aldrich, Saint Louis, MO, USA) assay was used to analyze the mitochondrial membrane potential (MMP). Cells were harvested by trypsinization, centrifuged, and the cells were suspended in 1 mL of Hanks′ Balanced Salt solution (HBSS; 14175095, Gibco, Paisley, UK) heated to 37°C. The samples were then centrifuged, 100 µL of 100 nM TMRE solution was added, and incubated (30 min, 37°C). To stop the reaction, 0.5 mL of HBSS buffer was added, and the cells were centrifuged. Finally, pellets were resuspended in 0.5 mL of HBSS, and MMP was measured by a Cytek Aurora™ flow cytometer (Cytek Biosciences, Fremont, CA, USA). Changes in mitochondrial potential were determined using Kaluza Analysis 2.2.1 software (Beckman Coulter, Bread, CA, USA).

Apoptosis Detection by Fluorescence Microscope

Nthy-ori 3–1 cells were seeded at a density of 2×10^4 cells/well onto coverslips placed in a 4-well plate and overnight at 37°C in 21% O_2 and 5% CO_2. The next day, the cells were treated to modify glycosylation and induce apoptosis as shown in Figure 2. On the fifth day, the cells were pre-fixed for 25 minutes in 4% formaldehyde cooled to 4°C. The cells were washed twice with PBS for 5 min. Permeabilization was performed in 0.2% Triton X-100 for 5 minutes at RT. To

remove the detergent, the cells were again washed with PBS. The cells on the coverslips were mounted in fluoroshield with DAPI (F6057, Sigma-Aldrich, Saint Louis, MO, USA), and gently transferred to the basic slide. Analysis of apoptosis was performed with an Eclipse E600 fluorescence microscope (Nikon, Tokyo, Japan) using DAPI blue fluorescence filters at 460 nm.

Statistical Analysis

The analysis of the obtained results was performed by the Brown-Forsythe and Welch one-way ANOVA test with Dunnett's T3 correction (MALDI-Tof MS) and the parametric one-way ANOVA test with Bonferroni correction (other analyses) in GraphPad Prism 9.5.1. Significance levels were denoted by symbols: */# for $p<0.05$ and **/# for $p<0.01$. The experiments were repeated at least three times.

Results

Previous research has already shown that the Fas protein undergoes *N*-glycosylation. Due to the predominance of complex-type structures in Fas glycoprotein,[30] to evaluate their role in the induction of cell death, we used Kf and Sw, the inhibitors of glycosylation, which block the *N*-glycan synthesis in the earliest stages of this process and prevent the formation of complex-type oligosaccharides (Figure 1).

Inhibitors of Glycosylation Do Not Affect the Viability and Protein Profiles of Nthy-Ori 3-1 Cells

The effect of glycosylation inhibitors on the viability of human thyrocytes was assessed by the alamarBlue assay. The following concentrations of Kf: 1, 5, 10, 25, 50, 75, and 100 µM (Figure 3A), and Sw: 1, 2.5, 5, 10, 25, 50, and 100 µg/mL (Figure 3B), as well as three times of treatment, were selected based on the previous research.[31,32]

The experiments have shown no statistically significant differences in the effects of both glycosylation inhibitors on thyroid epithelial cell viability in any of the tested variants (Figure 3A and B). The lack of effect of Kf and Sw at the selected concentrations on cell viability was a prerequisite for testing the efficacy of inhibitors in arresting *N*-glycosylation of Nthy-ori 3–1 cells at the stage of oligomannose structures in the case of Kf, and oligomannose/hybrid-type structures in the presence of Sw, to obtain a cell culture model for an evaluation of the importance of complex-type *N*-glycans in Fas-dependent apoptosis.

Coomassie brilliant blue staining of proteins resolved by SDS-PAGE was performed to evaluate the effect of glycosylation inhibitors on protein expression. We did not observe changes between protein profiles obtained for Kf- and Sw-treated Nthy-ori 3–1 cells (Figure 3C).

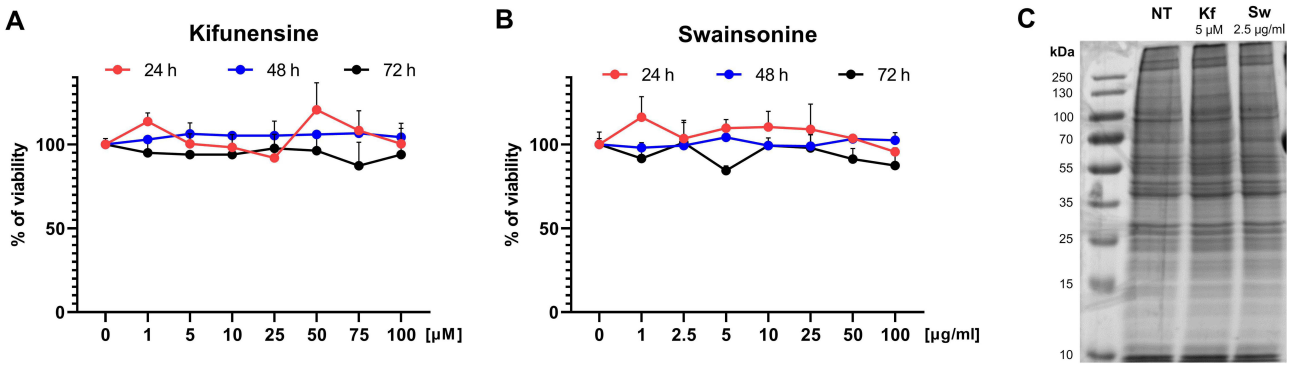

Figure 3 Effects of different concentrations of inhibitors on the viability and protein profiles of thyrocytes. (**A** and **B**) Nthy-ori 3–1 cells were treated with glycosylation inhibitors for 24 h (red lines), 48 h (blue lines), and 72 h (black lines), and the viability was determined by alamarBlue. The results were expressed as mean ± SD. The statistical analysis was performed using one-way ANOVA with Bonferroni correction. (**C**) Proteins extracted from non-treated (NT), as well as swainsonine- and kifunesine-treated cells (in the concentrations selected for the evaluation of apoptosis; 5 µM Kf, 2.5 µg/mL Sw) were separated by electrophoresis and stained with Coomassie Brilliant Blue.

Glycosylation Was Altered by the Inhibitors and FasL-Induced Apoptosis

MALDI-Tof mass spectrometry with sialic acid derivatization was applied for detailed qualitative and quantitative analysis of *N*-oligosaccharides. Glycans measured in positive ion reflectron mode were identified by their observed *m/z* values. The Symbol Nomenclature for Glycans (SNFG) notation was used to represent *N*-oligosaccharides graphically.[33] The relative intensities of each sugar structure were determined using the area under the peak calculation.

MALDI-Tof MS was useful for assessing the effectiveness of glycosylation inhibitors and the selection of their appropriate dose for apoptosis tests. Figure 4 shows the representative MALDI-Tof mass spectra for non-treated cells and the cells cultured in the presence of the glycosylation inhibitors in concentrations 5 µM for Kf and 2.5 µg/mL for Sw, chosen for the apoptosis assays. Among the tested concentrations in the range of 1–100 µM, 5 µM was the lowest dose of Kf giving the expected effect, and in the case of Sw 2.5 µg/mL was the lowest effective concentration from the range of 1–100 µg/mL. Kf in the concentrations of 5 µM stops *N*-glycosylation of Nthy-ori 3–1 thyrocytes at the stage of oligomannose structures, and 2.5 µg/mL of Sw accumulates oligomannose and hybrid-type *N*-glycans preventing the formation of complex-type structures (Figure 4). Kf and Sw inhibitory effect on glycosylation of Nthy-ori 3–1 cells was also confirmed by lectin blotting with the use of *Galanthus nivalis* lectin (GNL) recognizing oligomannose structures, and *Phaseolus vulgaris* lectin (PHA-L) specific for tri- and tetraantennary complex-type *N*-glycans (data not shown).

Mass spectrometry analysis was also performed for an evaluation of *N*-glycosylation changes in Nthy-ori 3–1 cells treated with IFNγ, a proinflammatory cytokine, and co-activated with IFNγ and FasL to induce apoptosis. For thyrocytes treated with

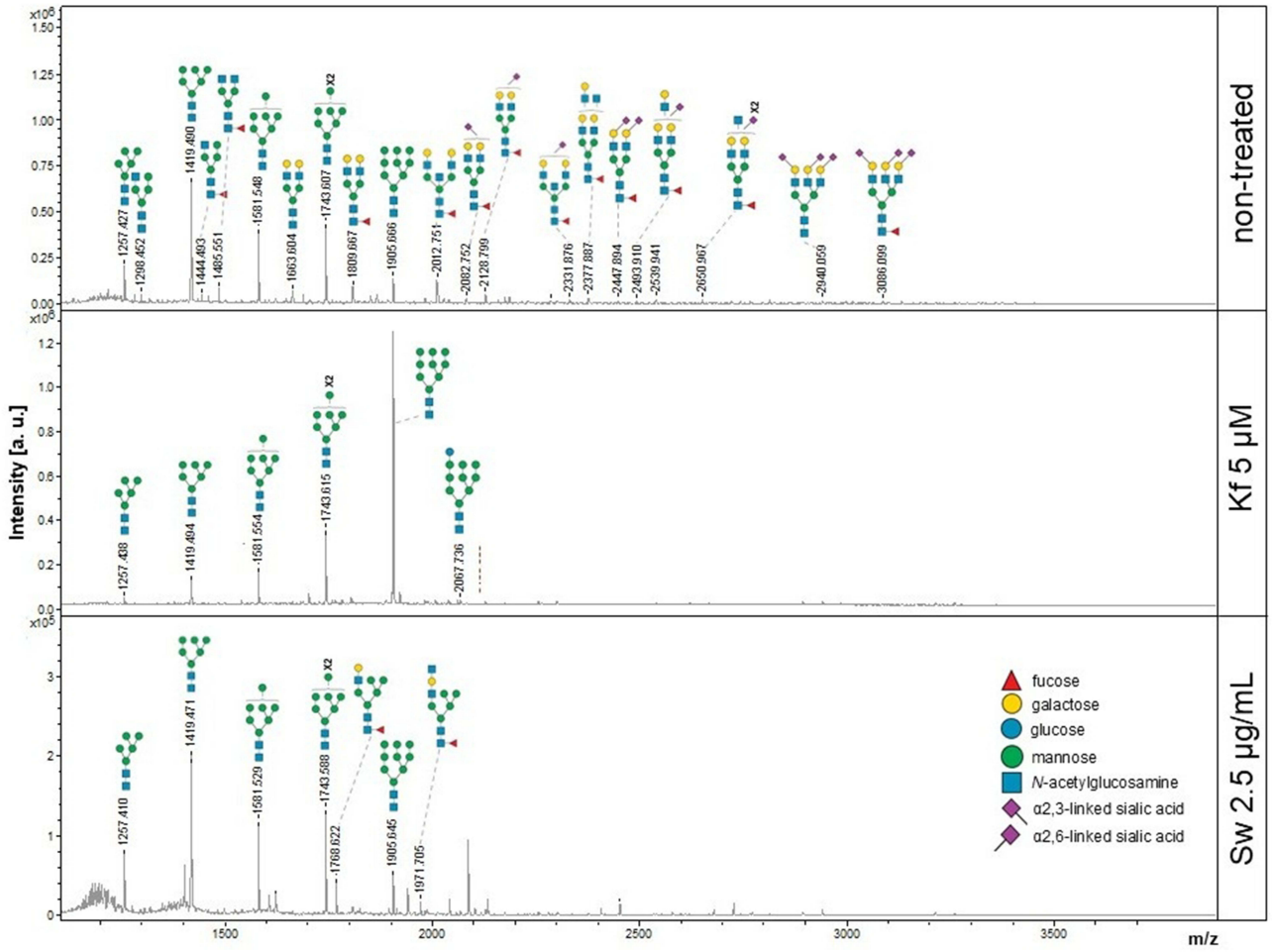

Figure 4 Representative mass spectra showing changes in *N*-glycosylation of thyrocytes treated with kifunensine and swainsonine. *N*-oligosaccharide samples were analyzed in positive ion reflectron mode.

Abbreviations: Kf, kifunensine; MALDI-Tof MS, matrix-assisted laser desorption/ionization with a time-of-flight analyzer mass spectrometry; *m*/z, mass to charge ratio; Sw, swainsonine.

https://doi.org/10.2147/JIR.S529858

IFNγ, IFNγ + FasL, and non-treated cells, 42 different *N*-glycan structures were identified (Figure 5 and Supplementary Table 1). In the MALDI-Tof mass spectra presented in Figure 4, the most abundant structures were depicted, while the detailed structural annotation of the oligosaccharides is summarized in Supplementary Table 1.

To quantitatively compare the abundance of the different forms of *N*-glycans, the obtained data was visualized as a color-coded heat map, in which all 42 oligosaccharide structures were collated (Figure 5A). The most intensive peaks within the glycome of the stimulated (IFNγ, and IFNγ + FasL) and non-treated cells were observed as high-mannose structures: H5N2, H6N2, H7N2, H8N2, and H9N2 (H, hexose; N, *N*-acetylhexosamine), with *m/z*: 1257.427, 1419.485, 1581.543, 1743.602 and 1905.660, respectively. Quantitative comparison of *N*-glycan groups revealed a significant increase of α2,3-sialylated glycan

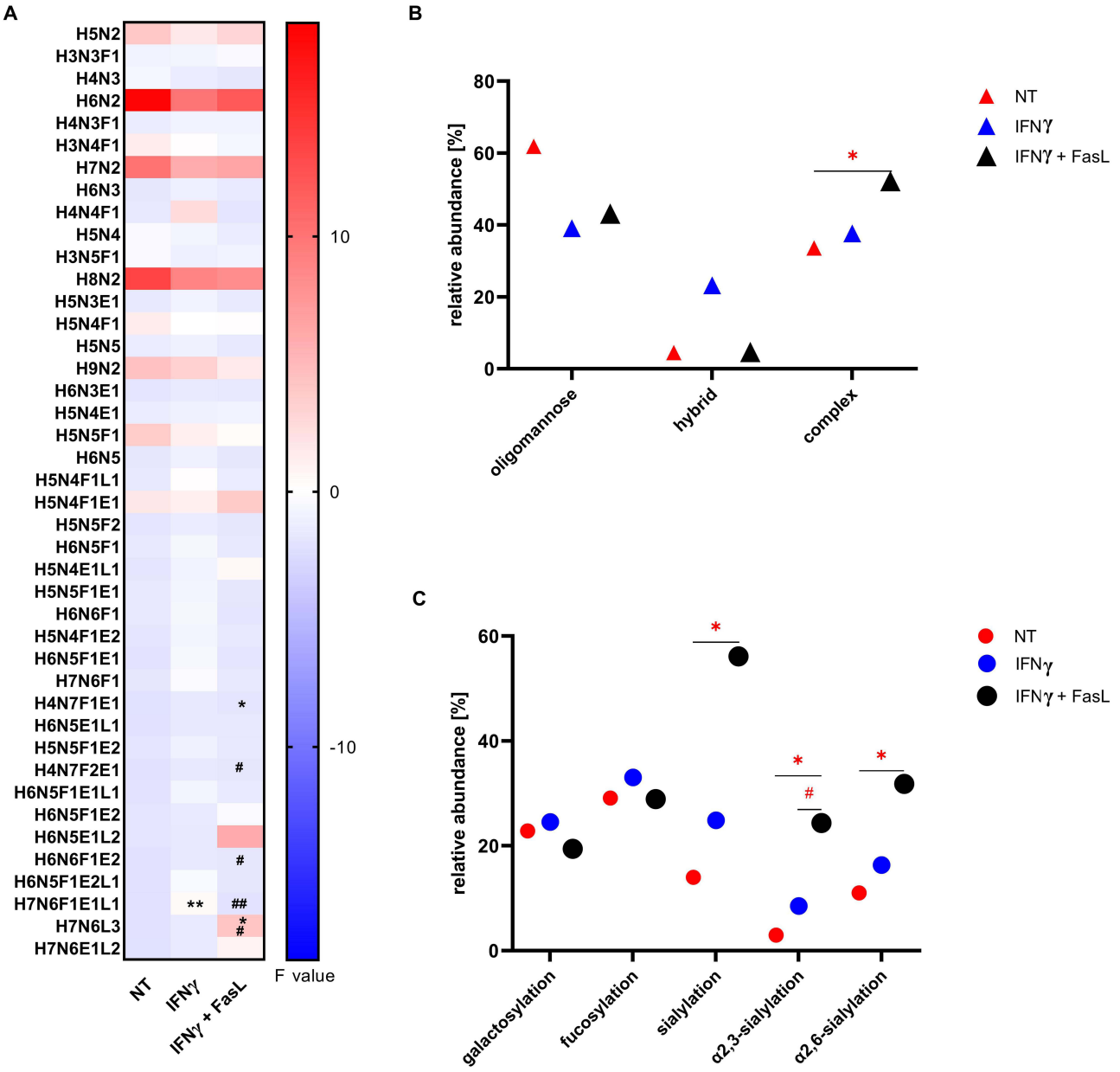

Figure 5 MALDI-Tof mass spectrometry analysis of *N*-glycans from Nthy-ori 3–1 thyrocytes with induced apoptosis. *N*-oligosaccharides were analyzed in positive ion reflectron mode. (**A**) Heatmap showing quantitative analysis of all structures detected by MALDI-Tof MS analysis. (**B**) Quantitative analysis for common structural features of *N*-glycans: fucosylation, galactosylation, α2,3-sialylation, and α2,6-sialylation. (**C**) Quantitative analysis for major glycan types: oligomannose, hybrid, and complex. The results are presented as mean values. The statistical significance was assessed using the Brown-Forsythe and Welch one-way ANOVA test with Dunnett T3 correction. Significance levels between treated cells (IFNγ and IFNγ + FasL) versus NT control are marked with asterisks as follows *p ≤ 0.05 and **p ≤ 0.01. Comparisons for treated cells IFNγ +FasL versus IFNγ are marked with crosses as follows $^{\#}p \leq 0.05$ and $^{\#\#}p \leq 0.01$.

Abbreviations: H, hexose; N, *N*-acetylhexosamine; F, fucose; E, ester; L, lactone; FasL, Fas ligand; IFNγ, interferon-gamma; NT, non-treated.

(H7N6L3, *m/z* 3213.136; L, lactone) in IFNγ + FasL-treated cells compared both to NT control, and IFNγ, as well as up-regulation of α2,6-sialylated structure (H4N7F1E1, *m/z* 2575.933; E, ester; F, fucose) in apoptotic cells versus untreated cells. Nthy-ori 3–1 cells co-treated with IFNγ and FasL also showed an increasing content of α2,6-sialylated *N*-glycans with two fucoses (H4N7F2E1, *m/z* 2721.960) or a single Fuc residue, and both α2,3- and α2,6-linkage SA (H6N5F1E2L1, *m/z* 3086.099) compared to IFNγ-stimulated thyrocytes. A statistically significant reduction of H7N6F1E1L1 glycoform at *m/z* 3132.156 was observed in IFNγ-stimulated cells in comparison to control, while co-treatment with FasL restored the amount of this *N*-glycan to the level of control (Figure 5A and Supplementary Table 1).

We also quantitatively compared the abundance of *N*-glycans assigned to the following subgroups: galactosylated, fucosylated, α2,3- and α2,6-sialylated (Figure 5B), as well as the main groups: oligomannose, hybrid-, and complex-type *N*-glycans. It was noted that the predominant type of *N*-oligosaccharide structures changed between the groups. In NT and IFNγ-treated cells, oligomannose structures predominated, while in IFNγ + FasL-treated cells with apoptotic phenotype, the level of complex-type structures increased, accounting for about 50% of the glycomic pool (Figure 5C). In addition, the analysis of *N*-glycan subgroups demonstrated an up-regulation of α2,3- and α2,6-sialylation in Nthy-ori 3–1 thyrocytes activated with IFNγ + FasL vs NT (Figure 5B). The content of α2,3-linked SA was also significantly higher in IFNγ + FasL-treated Nthy-ori 3–1 thyrocytes compared to IFNγ-stimulated cells (Figure 5B).

Complex-Type *N*-Glycans Play a Role in Fas/FasL-Induced Apoptosis of the Nthy-Ori 3-1 Cell Line

The importance of complex-type *N*-glycans in Fas/FasL-induced apoptosis of Nthy-ori 3–1 cell line was determined for Kf- and Sw-treated cells using four apoptosis tests at different stages of this process. A more than 2-fold increase in Fas protein expression on the surface of thyrocytes after IFNγ treatment was determined by flow cytometry. Importantly, the glycosylation inhibitors did not affect the surface expression of Fas (Figure 6). Thus, we can assume that the changes in thyrocyte apoptosis described below result only from the altered glycosylation of Fas but not from its amount on the cell surface.

Swainsonine Decreases Nthy-Ori 3-1 Apoptosis at an Early Stage

At first, an Annexin V assay to evaluate phosphatidylserine externalization, and a Caspase 3 and 7 Detection Kit to assess the activity of caspases 3 and 7 were used. The percentage of early-apoptotic and late-apoptotic human thyrocytes, as well as necrotic cells, was determined by flow cytometry (Figures 7A, B and 8A, B).

As expected, exposure of Nhty-ori 3–1 cells to FasL resulted in a significant up-regulation of apoptotic cells. We observed an approximately 10-fold increase in the number of annexin V-FITC+ PI- cells (Figure 7B) and a 3-fold rise in the number of Casp 3/7+ Sytox- thyrocytes (Figure 8B) co-treated with IFNγ and FasL compared to NT. Similarly, the percentage of thyrocytes with an active Casp 3/7 was about 2-fold higher in FasL-treated cells (INFγ + FasL) than in NT cells.

Interestingly, the results of both assays showed a Sw-dependent decrease in the number of early apoptotic cells (Figure 7) and the cells with active caspase 3/7 (Figure 8) in comparison to Nthy-ori 3–1 cells co-treated with IFNγ and FasL, up to the level of NT cells. The reduction of the early apoptotic cells in the presence of Sw (IFNγ + FasL + Sw) was as much as 2-fold compared to the control variant (IFNγ + FasL) (Figures 7B and 8B). In the case of Casp 3/7 activity, we observed the down-regulation in Sw-treated cells compared to the INFγ+/FasL+ variant, both in Casp 3/7+ Sytox- (early apoptosis) and Casp 3/7+ Sytox+ (late apoptosis) cells.

The number of late-apoptotic cells (annexin V-FITC+ PI+) has not changed in the presence of both glycosylation inhibitors (IFNγ + FasL + Kf, IFNγ + FasL + Sw) vs IFNγ + FasL control variant, while was statistically higher compared to NT cells (Figure 7).

Inhibitors of Glycosylation Restore Mitochondrial Potential in Nthy-Ori 3-1 Cells

To identify the influence of glycosylation inhibitors on mitochondrial membrane potential, Nthy-ori 3–1 cells were stained with TMRE and analyzed using a flow cytometer. The incubation of cells with INFγ and FasL induced significant depolarization of mitochondrial membranes compared to NT cells. The exposure of thyrocytes to both IFNγ + FasL + Kf

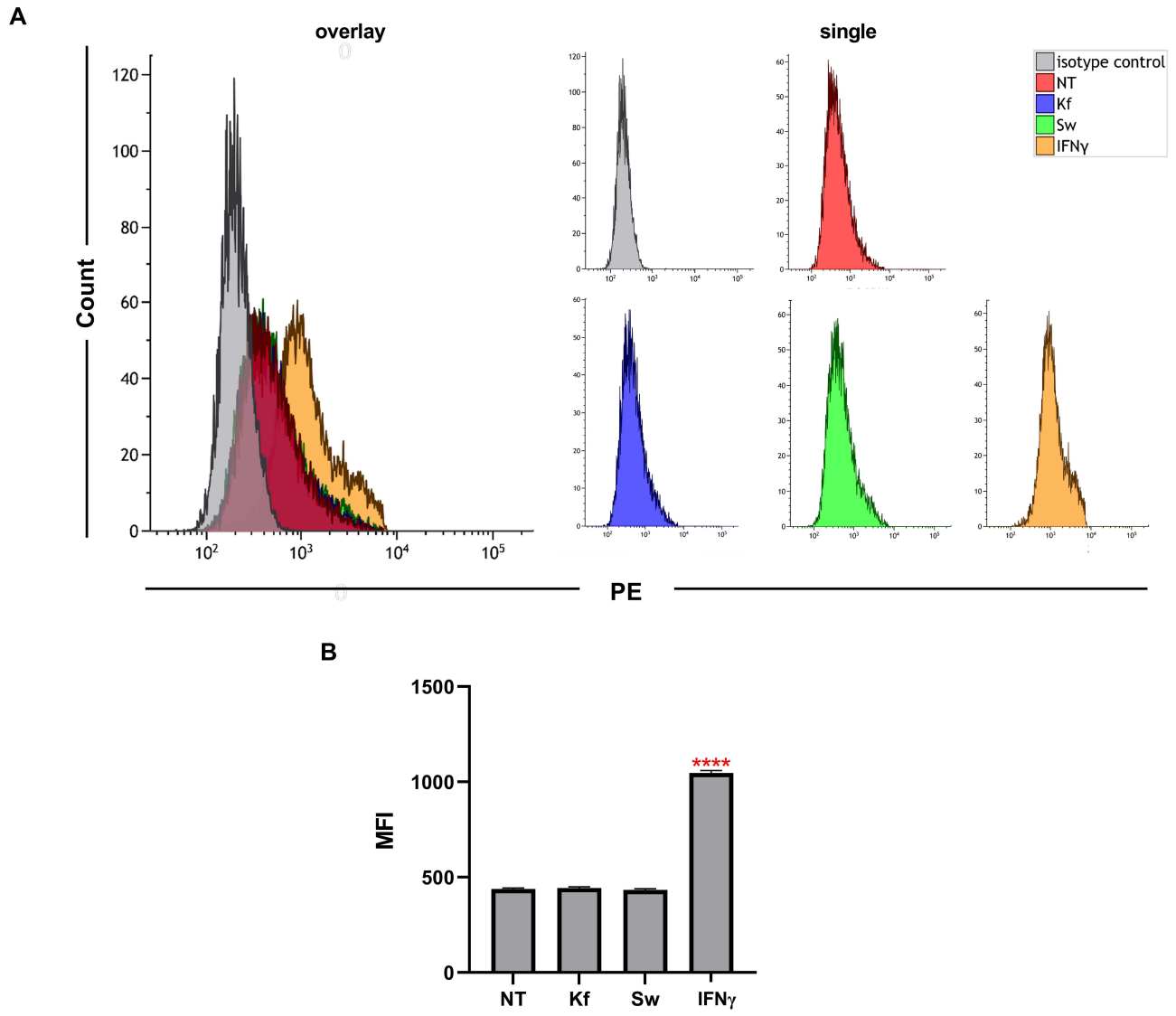

Figure 6 Evaluation of Fas expression on Nthy-ori 3–1 thyrocyte surface with glycosylation inhibitors for 72 h. Analysis was performed using PE-conjugated anti-Fas IgG1 by flow cytometry. (**A**) Representative overlay and single histograms. (**B**) Cumulative bar graph for MFI values. Results are expressed as mean ± SD. The statistical significance of the data was assessed using one-way ANOVA with Bonferroni correction. Statistical significance between IFNγ-treated cells and NT cells is indicated with asterisks as follows: ****p ≤ 0.0001.

Abbreviations: IFNγ, interferon-gamma; Kf, kifunensine; MFI, mean fluorescence intensity; NT, non-treated; PE, phycoerythrin; Sw, swainsonin.

and IFNγ + FasL + Sw resulted in an increased percentage of cells with high MMP compared to INFγ + FasL control. The changes of glycosylation in Kf- and Sw-treated thyrocytes restored the effect of IFNγ + FasL on mitochondrial potential to the level of NT cells (Figure 9A and B).

Fragmentation of Nuclei Was Reduced in Swainsonine-Treated Nthy-Ori 3-1 Cells

The influence of glycosylation inhibitors on Nthy-ori 3–1 apoptosis via the Fas/FasL pathway was also analyzed in terms of the morphology of the nucleus by fluorescence visualization after DAPI staining. Fragmentation of nuclei and formation of apoptotic bodies were noticed in Nthy-ori 3–1 cells treated with IFNγ + FasL and the variant with Kf (IFNγ + FasL + Kf) (Figure 10, red arrows). The number of fragmented/shrunken cell nuclei was lower in Sw-treated cells than in the reference IFNγ + FasL variant. This observation was consistent with the above-described results obtained by flow cytometry, which showed the lower externalization of phosphatidylserine and caspase activity in the

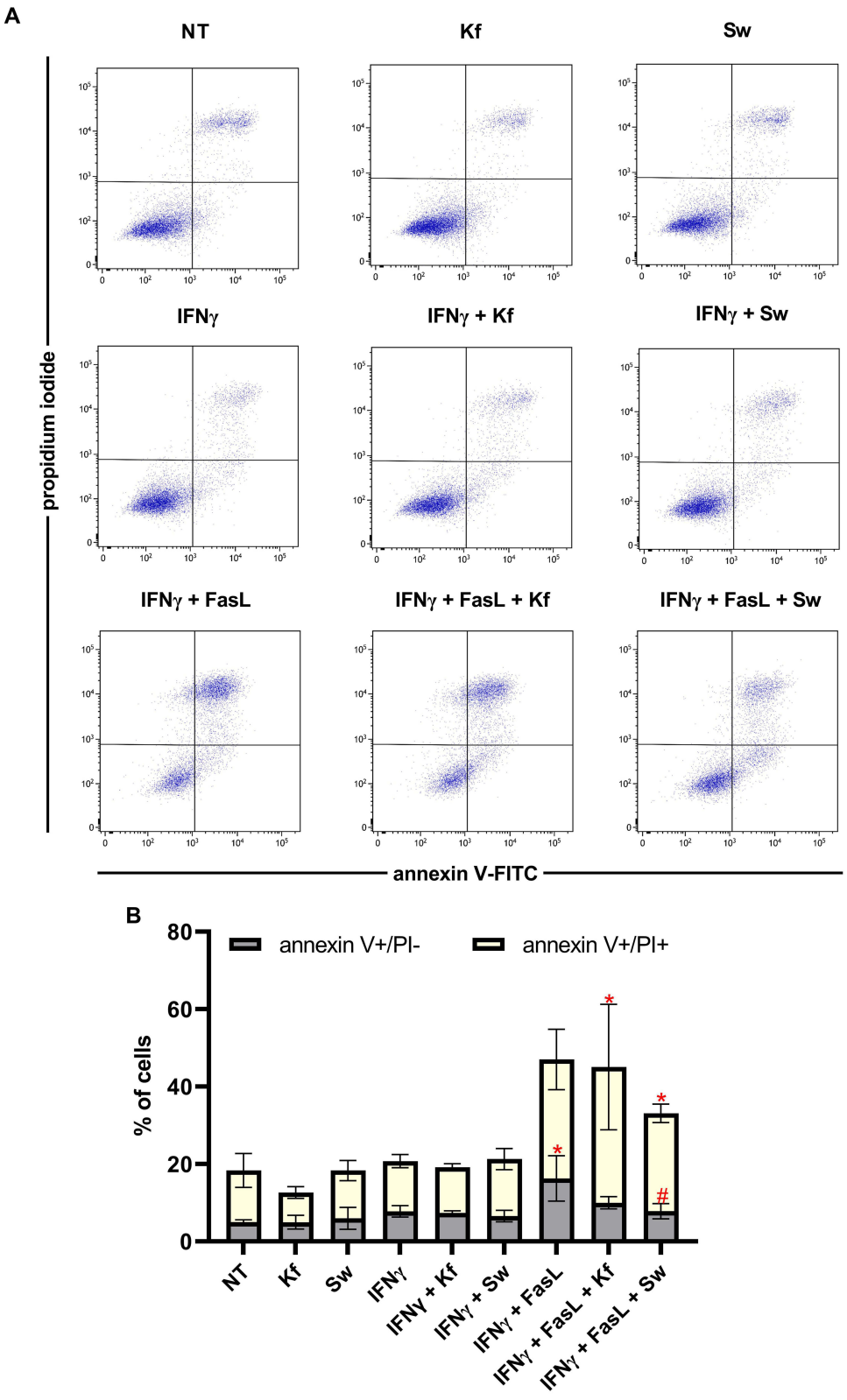

Figure 7 Detection of apoptosis in Nthy-ori 3–1 cell line treated with glycosylation inhibitors for 72 h. Human recombinant IFNγ (20 ng/mL) stimulated Fas expression, and human recombinant FasL (20 ng/mL) induced thyrocyte apoptosis, which was determined by annexin V-FITC staining in flow cytometry. (**A**) Representative dot plots for all tested variants. (**B**) Stacked bar graph for % Annexin V-FITC+ PI- (early apoptosis) and Annexin V-FITC+ PI+ (late apoptosis) cells. The results are shown as mean values ± SD. The statistical analysis was performed using one-way ANOVA with Bonferroni correction. Statistical significance between IFNγ + FasL-treated cells vs NT cells is marked with asterisks as follows * $p \leq 0.05$, and between Kf- and Sw-treated cells in apoptotic variants (IFNγ +FasL + Kf; IFNγ +FasL + Sw) relative to apoptotic cells with unmodified glycosylation (IFNγ +FasL) is marked with crosses as follows $^{\#}p \leq 0.05$.

Abbreviations: FasL, Fas ligand; IFNγ, interferon-gamma; Kf, kifunensine; NT, non-treated; Sw, swainsonine.

https://doi.org/10.2147/JIR.S529858

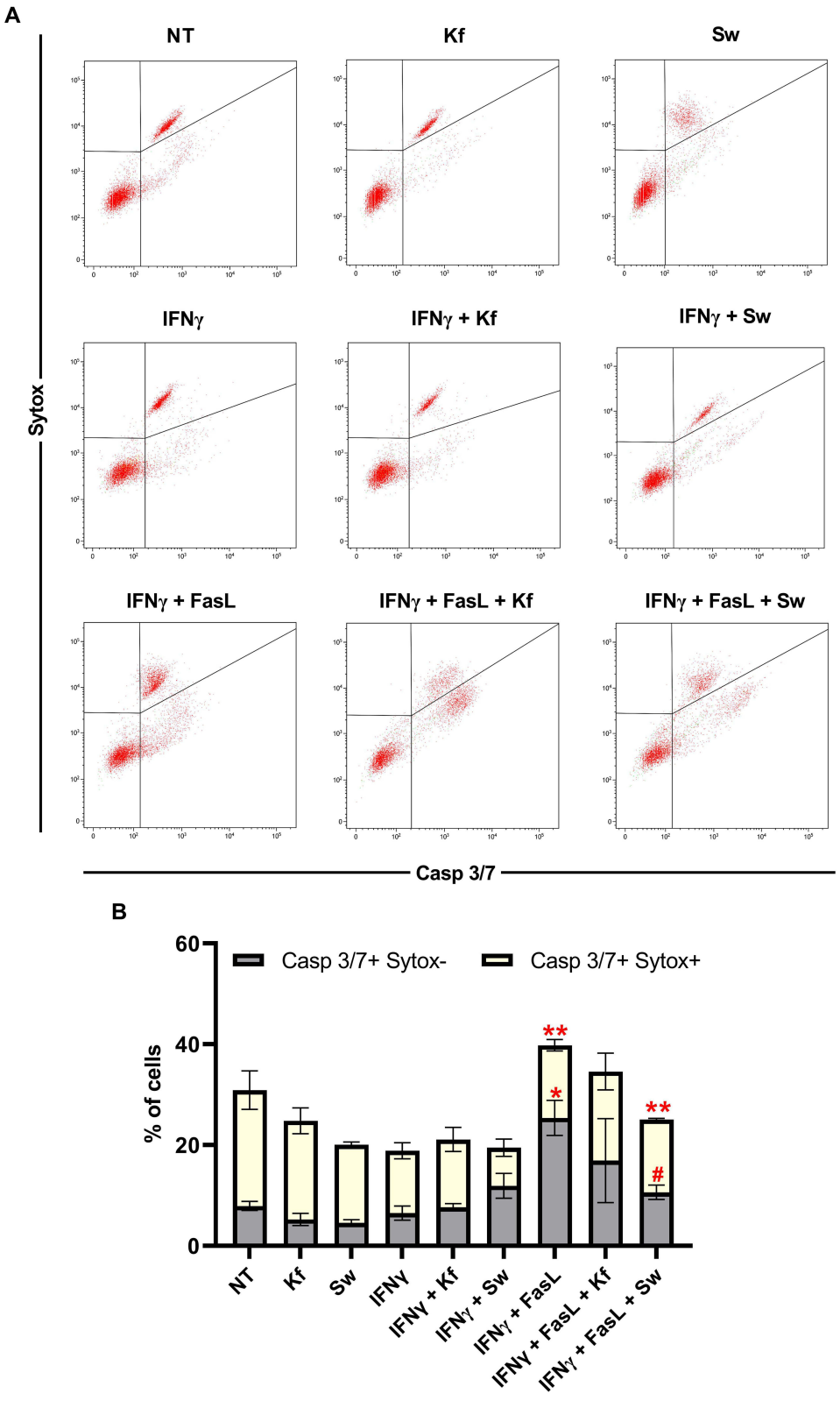

Figure 8 Detection of Casp 3/7 activity in thyrocytes treated with glycosylation inhibitors for 72 h. Human recombinant IFNγ (20 ng/mL) stimulated Fas expression, and human recombinant FasL (20 ng/mL) induced thyrocyte apoptosis, which was determined using the CellEvent™ Caspase 3/7 Green Flow Cytometry Detection Kit in flow cytometry. (**A**) Representative dot plots for all tested variants. (**B**) Cumulative bar graph for % of Casp 3/7+ Sytox- and Casp 3/7+ Sytox+ cells. The results are shown as mean values ± SD. The statistical analysis was performed using one-way ANOVA with Bonferroni correction. Statistical significance between IFNγ + FasL-treated cells vs NT cells are marked with asterisks as follows: * $p \leq 0.05$; ** $p \leq 0.01$, and between Kf- and Sw-treated cells in apoptotic variants (IFNγ +FasL + Kf; IFNγ +FasL + Sw) relative to apoptotic cells with unmodified glycosylation (IFNγ +FasL) is marked with crosses as follows $^{\#}p \leq 0.05$.
Abbreviations: FasL, Fas ligand; IFNγ, interferon-gamma; Kf, kifunensine; NT, non-treated; Sw, swainsonine.

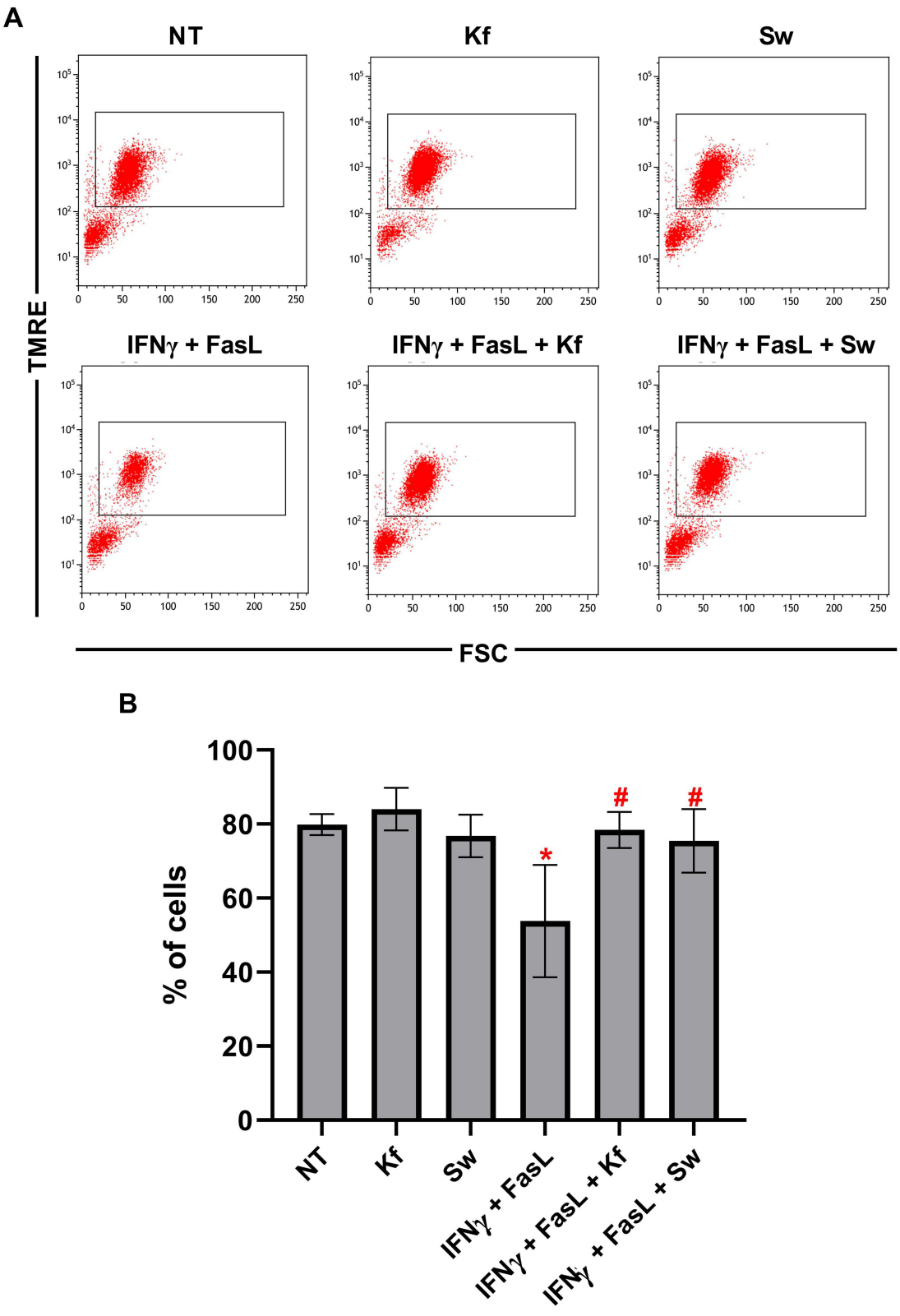

Figure 9 Effect of glycosylation inhibitors on mitochondrial membrane potential in the Nthy-ori 3–1 cell line. Human recombinant IFNγ (20 ng/mL) stimulated Fas expression and human recombinant FasL (20 ng/mL) induced thyrocyte apoptosis. Cells were stained with TMRE and analyzed by flow cytometry. (**A**) Representative dot plots showing the gated Nthy-ori 3–1 cells with the high MMP. (**B**) Bar graph for % of thyrocytes with the high MMP. The results are shown as mean values ± SD. The statistical analysis was performed using one-way ANOVA with Bonferroni correction. Statistical significance between IFNγ + FasL-treated cells vs NT is marked with asterisks as follows * $p \leq 0.05$, and between Kf- and Sw-treated cells in apoptotic variants (IFNγ +FasL + Kf; IFNγ +FasL + Sw) relative to apoptotic cells with unmodified glycosylation (IFNγ +FasL) are marked with crosses as follows $^{\#}p \leq 0.05$.

Abbreviations: FasL, Fas ligand; IFNγ, interferon-gamma; Kf, kifunensine; MMP, mitochondrial membrane potential; NT, non-treated; Sw, swainsonine; TMRE, tetramethylrhodamine ethyl ester perchlorate.

https://doi.org/10.2147/JIR.S529858

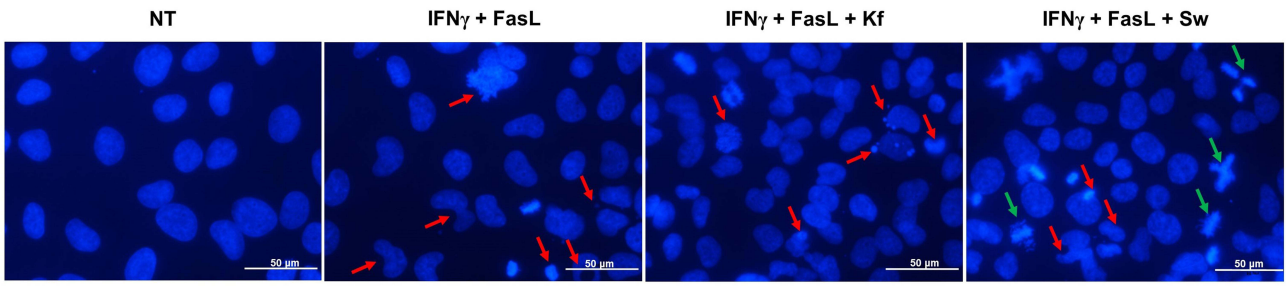

Figure 10 Effect of glycosylation inhibitors on the morphology of cell nuclei of thyrocytes. Human recombinant IFNγ (20 ng/mL) stimulated Fas expression and human recombinant FasL (20 ng/mL) induced thyrocyte apoptosis. Cells were stained with DAPI and analyzed in fluorescence microscopy. Red arrows show fragmented cell nuclei and apoptotic bodies, green arrows indicate cellular divisions of the nucleus.
Abbreviations: FasL, Fas ligand; IFNγ, interferon-gamma; Kf, kifunensine; NT, non-treated; Sw, swainsonine.

presence of Sw (Figures 5 and 6). In addition, numerous mitotic divisions of cell nuclei were observed in Sw-treated cells (Figure 10, green arrows).

Discussion

Fas-mediated apoptosis is a physiological process necessary for the proper development of the organism. However, disturbances in this process can promote the development of various pathologies, including autoimmune diseases and cancer.[34–36] Among the endogenous factors regulating apoptosis, the glycosylation of the death receptors seems to play an essential role in both maintaining their activity as well as interactions with ligands, and finally, the generation of death signals.[11,37] The involvement of *N*-glycosylation in the regulation of Fas signaling remains a topic of considerable debate. One hypothesis suggests that Fas *N*-glycans, among which complex-type structures predominate, are required for FasL binding.[38] The proximity of the N136 and N118 glycosylation sites in the extracellular domain to the ligand-binding site suggests that Fas *N*-glycans could directly influence Fas/FasL interactions or modify the conformation of this region. Such changes may regulate FasL binding, thereby directly impacting the Fas-dependent cellular response.[11]

Apoptosis via Fas/FasL-mediated signaling is a way of thyrocyte elimination and thyroid destruction in Hashimoto's thyroiditis.[10] Proinflammatory cytokines, like IFNγ, are produced abundantly by immune cells in the thyroid gland in HT,[9] and stimulate the expression of Fas in thyrocytes, which makes them susceptible to apoptosis[10] induced by FasL present on immune cells, mainly T cells infiltrating the thyroid gland.[39] Proinflammatory cytokines, apart from the main function of inducing and maintaining chronic inflammation, were shown to alter the biosynthesis of *N*-glycans.[40] Inflammation of the thyroid gland, characteristic of HT, may affect the glycosylation of thyrocytes, which in turn may contribute to the destruction of the thyroid follicles. These are the reasons why we focused this research on the importance of *N*-glycans in Fas-mediated apoptosis of the human thyrocytes.

We established an in vitro model of HT using human thyroid follicular epithelial cells (Nthy-ori 3–1 cell line). IFNγ was successfully served to stimulate Fas expression, and human recombinant FasL-induced thyrocyte apoptosis (Figures 7 and 8). IFNγ has been previously used to promote the expression of death receptors. Research on the human QBC939 biliary tract cancer cell line has shown the ability of IFNγ to increase Fas and FasL expression,[35] and in the study on the primary culture of thyrocytes, up-regulation of Fas expression was observed in the presence of IFNγ.[41]

Different approaches have been applied to assess the importance of glycan structures in receptor activity. Downregulation or overexpression of glycosyltransferase, responsible for a single reaction resulting in adding a specific monosaccharide, is commonly used to determine the role of oligosaccharides modified by this glycosyltransferase. Overexpression and silencing of the gene encoding ST6Gal-I enzyme in mouse monocytes showed the key role of α2,6-sialylated *N*-oligosaccharides in the control of programmed cell death.[42] The use of glycosylation inhibitors allows blocking this process at a given stage of synthesis, preventing the presence of a specific type of structure on glycoconjugates. This approach was useful in our study to eliminate complex-type structures from Fas to determine their role in apoptosis-inducing signals.

Our study showed consistently with the use of different assays that co-treatment with IFNγ and FasL significantly increases Fas-mediated apoptosis manifested at the early stage by the intense externalization of phosphatidylserine (Figure 7), the up-regulated activity of caspases 3 and 7 (Figure 8), and finally by shrinking of cell nuclei and formation of apoptotic bodies (Figure 10). Importantly, Nthy-ori 3–1 cells stimulated with IFNγ and FasL showed a higher level of complex-type *N*-oligosaccharides (Figure 5B), and within them α2,3- and α2,6-sialylated structures (Figure 5C) compared to untreated and IFNγ-stimulated cells, which could confirm the necessity of these oligosaccharides to bind ligand and activate the Fas receptor.

Since swainsonine did not affect the viability of Nthy-ori 3–1 thyrocytes (Figure 3A and B), the changes we observed in Figures 7–10 are likely due to a direct effect of this glycosylation inhibitor on the apoptotic pathway. A lack of complex-type structures in Sw-treated Nthy-ori 3–1 cells resulted in the decreased number of early-apoptotic cells (Figure 7), caspase activity (Figure 8), restored mitochondrial membrane potential (Figure 9), and less fragmentation of cell nuclei (Figure 10) in response to FasL. Oligomannose/hybrid-type *N*-oligosaccharides on Fas, formed in the presence of Sw, are probably not optimal to bind FasL or a functional spatial Fas structure, and the replacement of complex-type structures by oligomannose/hybrid-type *N*-glycans decreases DISC cross-linking by hindering procaspase-8 oligomerization between adjacent death receptor complexes.[38] Our results are related to the previously published data by Lv et al, which showed a reduced oligomerization of Fas in response to FasL in LPS (lipopolysaccharide)-stimulated H9c2 rat embryonic cardiomyocyte cells with Sw-modified glycosylation, and reduced expression of BAX protein, cleaved caspases 3 and 9.[43] These reports, obtained for different types of cells, demonstrate the importance of Fas *N*-glycans in receptor oligomerization, which in turn is necessary to generate an intracellular signal. In addition, Sw was shown to down-regulate cytochrome c release and reduce mitochondrial depolarization.[44] Mitochondria are crucial in cell death signaling, with changes in their function occurring during the early phases of apoptosis. Sw can restore mitochondrial membrane potential and thus prevent apoptosis.[7]

An important modification of complex-type *N*-glycans is the addition of α2,3- and α2,6-SA to the antennae. It has been observed that Fas is a highly sialylated glycoprotein.[30] Our study demonstrated the statistically significant increase of α2,3- or α2,6-sialylated structures (H4N7F1E1, H4N7F2E1, H6N5F1E2L1, H7N6F1E1L1, and H7N6L3) in Nthy-ori 3–1 cells co-treated with IFNγ and FasL relative to NT and IFNγ-stimulated cells (Figure 5A). It was shown both for α2,3- and α2,6-sialylation analyzed separately, and for the total sialylation (Figure 5B). This allows us to conclude that the up-regulation of sialylation correlates with a boost in apoptosis of IFNγ + FasL-treated follicular thyroid cells (Figures 7–10). Sw preventing the formation of complex-type structures also significantly reduces sialylation (Figure 4), which may result in a decrease in Fas oligomerization. Interestingly, the removal of sialic acid residues from *N*-glycan structures using α2,3/6/8-sialidase from *Vibrio cholerae* does not entirely prevent FADD recruitment to the DISC and leads to only a partial reduction in procaspase-8 activation within the DISC complex.[38] Recent studies have shown that α2,6-sialylation of Fas does not interfere with the ligand binding but inhibits DISC complex formation and internalization of this receptor. A total desialylation of Fas glycans using the neuraminidase from *Vibrio cholerae* increases the sensitivity of T and B lymphocytes to Fas/FasL-induced apoptosis.[16] Thus, the degree of Fas sialylation seems to be another checkpoint in the regulation of cell death through the Fas/FasL signaling pathway. Nevertheless, the detailed mechanisms of the role of Fas sialylation in apoptosis still need to be discovered due to the complexity of this process resulting from the different glycosidic bonds and SA negative charge.[11,45–47]

The effect of swainsonine and kifunesine activity on *N*-glycan biosynthesis is quite similar, both inhibitors prevent the formation of complex-type structures, but Kf inhibits α-mannosidase I which acts before α-mannosidase II blocked by Sw resulting in only oligomannose structures in case of Kf, and oligomannose/hybrid-type *N*-glycans in the presence of Sw (Figure 1). Despite the similar effects of their activity, we observed the different responses of Nthy-ori 3–1 to Fas-mediated signals in the presence of Kf and Sw in three of four performed tests (Figures 7, 8 and 10). What is interesting is that similar results were obtained in other studies. Treatment of HeLa cells with 1-deoxynojirimycin, which, like Kf, blocks the action of α-mannosidase I, caused a slight decrease in FADD and procaspase 8 activity,[38] which may indicate that oligomannose structures are not suitable for Fas oligomerization. We can speculate about the key role of the monosaccharides building the outer parts, called antennas in the complex-type *N*-glycans, like galactose, fucose, and sialic acid, by referring to the results obtained for Sw in the regulation of Fas-mediated signal transduction (Figure 11).

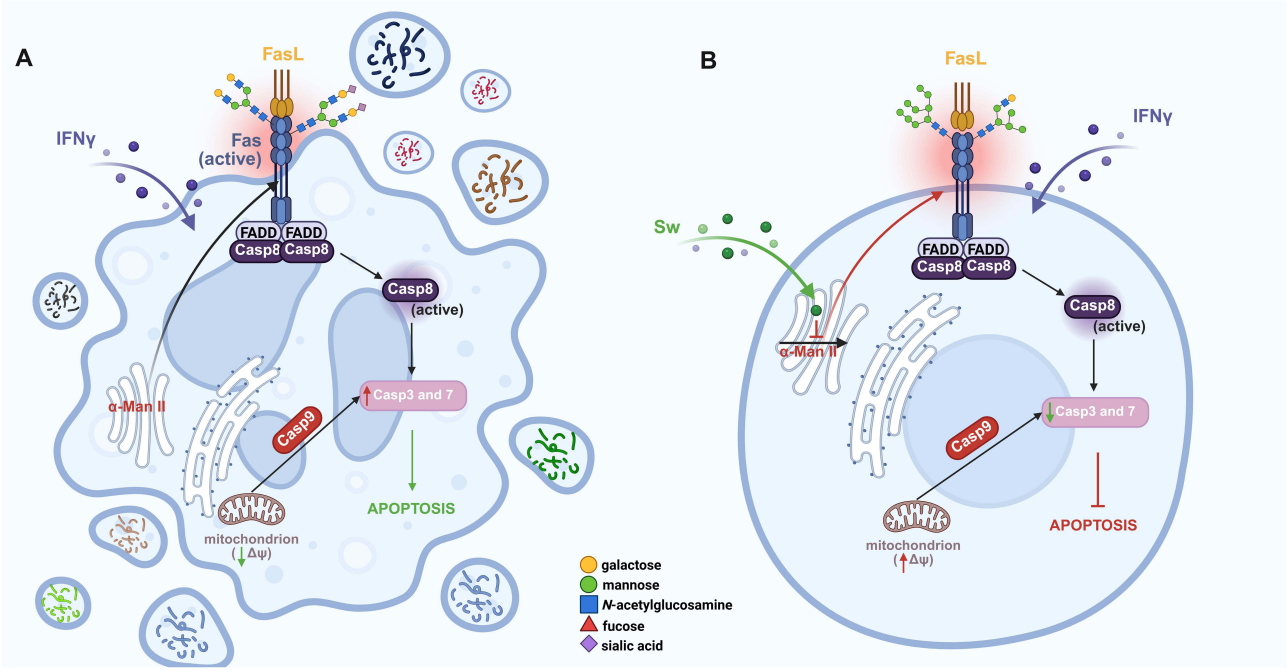

Figure 11 Proposed mechanism of swainsonine regulation of Fas-mediated apoptosis in Nthy-ori 3–1 thyrocytes. (**A**) In Sw-untreated thyrocytes, *N*-glycosylation reaches the final stage of complex-type structures, which are attached to Fas predominantly. Complex-type *N*-glycans on Fas are crucial to generating intracellular signals resulting in apoptosis. (**B**) Sw blocks α-Man II at the rough endoplasmic reticulum which leads to the attaching of oligomannose and hybrid-type *N*-glycans to Fas. The signal generated by Fas-FasL interaction is significantly lowered which prevents thyrocytes from apoptosis. Created in BioRender. Trzos, S. (2025) https://BioRender.com/s03e383.
Abbreviations: α-Man II, α-mannosidase II; Casp, caspase; FADD, Fas-associated death domain; FasL, Fas ligand; IFNγ, interferon-gamma; Sw, swainsonine.

Moreover, it is worth noting that the intrinsic and extrinsic pathways of programming cell death are interconnected[11] which may explain the statistically significant restoration of mitochondrial membrane depolarization by Kf (Figure 9). It seems that Kf could affect cell death independently of the caspase cascade by decreasing the production of proapoptotic proteins BAX and BAK, resulting in increased mitochondrial potential. However, the effect of Kf on thyrocytes needs further verification.

Conclusions

In conclusion, the present study demonstrated a key effect of the Sw-blocked glycosylation on the regulation of apoptosis through the Fas/FasL pathway in human thyroid cells of the Nthy-ori 3–1 cell line. The protective effect of Kf was not confirmed in each applied assay. This is the first report to highlight the use of Sw as a potential inhibitor of thyroid apoptosis in vitro, which only emphasizes that the presence of complex-type *N*-glycan structures is responsible for Fas/FasL signaling. Further studies are needed to deeply explore the mechanism of Sw activity on the Fas-trigger signaling pathway. The anti-apoptotic potential of swainsonine has to be validated on other research models, in particular in vivo animal studies are necessary to determine the highly probable side effects due to the wide range of Sw biological effects.

The obtained results are important in the context of autoimmune thyroid diseases, particularly Hashimoto's thyroiditis, where destruction of the gland mainly results from the activation of the Fas/FasL signaling pathway and leads to hypothyroidism with serious consequences for the whole body. Our study is a very potent dataset as a basis for further studies to determine the influence of the specific glycosylation changes of apoptotic proteins, such as Fas, on their biological functions in thyrocytes to address questions on the mechanism of the intensified apoptosis in Hashimoto's thyroiditis. Profiling of thyrocyte proteome, which is sensitive to Sw to select glycoproteins for further functional analysis of the effects of Sw-altered glycosylation, is also one of the required future directions.

Abbreviations

Asn, asparagine; BCL-2, B-cell lymphoma 2; BID, BH3 interacting-domain; Casp, caspase; DISC, death-inducing signaling complex; FADD, Fas-associated death domain; FasL, Fas ligand; Fuc, fucose; GA, Golgi apparatus; GlcNAc, *N*-acetylglucosamine; HT, Hashimoto's thyroiditis; IFNγ, interferon-gamma; Kf, kifunensine; MALDI-ToF MS, matrix-assisted laser desorption/ionization with a time-of-flight analyzer mass spectrometry; Man, mannose; MOMP, mitochondrial outer membrane permeabilization; RER, rough endoplasmic reticulum; SA, sialic acid; ST, sialyltransferase; Sw, swainsonine; TMRE, tetramethylrhodamine ethyl ester perchlorate.

Data Sharing Statement

The raw data obtained in this study are available in the RODBUK Cracow Open Research Data Repository (https://uj.rodbuk.pl/), doi.org/10.57903/UJ/USTLJE.

Acknowledgments

The authors thank Professor Anna Pecio (Department of Comparative Anatomy, Institute of Zoology and Biomedical Research, Faculty of Biology, Jagiellonian University, Krakow, Poland) for access to the fluorescence microscope. We also wish to acknowledge Natalia Wojtowicz for her participation in the preliminary study, which is not included in this paper. The study was carried out with the use of equipment co-financed by the qLIFE and BioS Priority Research Area under the program "Excellence Initiative – Research University" at Jagiellonian University in Kraków, Poland, and research infrastructure co-financed by the Smart Growth Operational Programme POIR 4.2 project no. POIR.04.02.00-00-D023/20. This publication has been supported by a grant from the Priority Research Area qLIFE under the Strategic Programme Excellence Initiative at Jagiellonian University. The graphical abstract was created in BioRender. Trzos, S. (2025) https://BioRender.com/i81c505.

Author Contributions

All authors made a significant contribution to the work reported, whether that is in the conception, study design, execution, acquisition of data, analysis and interpretation, or in all these areas; took part in drafting, revising or critically reviewing the article; gave final approval of the version to be published; have agreed on the journal to which the article has been submitted; and agree to be accountable for all aspects of the work.

Funding

The research has been funded by grant No. U1U/P03/NO/03.28 from the Priority Research Area under the Strategic Programme Excellence Initiative at the Jagiellonian University. The purchase of the Cytek Aurora™ flow cytometer was supported by grant from the Priority Research Area (BioS) under the Strategic Programme Excellence Initiative at the Jagiellonian University.

Disclosure

The abstract of this paper was presented at the 19th World Immune Regulation Meeting (Switzerland, Davos) as a poster presentation with interim findings. The authors report no conflicts of interest in this work.

References

1. Eguchi K. Apoptosis in autoimmune diseases. *Internal Medicine*. 2001;40:275–284. doi:10.2169/internalmedicine.40.275
2. Elmore S. Apoptosis: a review of PROGRAMMED CELL DEATH. *Toxicol Pathol*. 2007;35:495–516. doi:10.1080/01926230701320337
3. Yonehara S. Death receptor Fas and autoimmune disease: from the original generation to therapeutic application of agonistic anti-Fas monoclonal antibody. *Cytokine Growth Factor Rev*. 2002;13:393–402. doi:10.1016/S1359-6101(02)00024-2
4. Bertheloot D, Latz E, Franklin BS. Necroptosis, pyroptosis and apoptosis: an intricate game of cell death. *Cell Mol Immunol*. 2021;18:1106–1121. doi:10.1038/s41423-020-00630-3
5. Xu X, Lai Y, Hua Z-C. Apoptosis and apoptotic body: disease message and therapeutic target potentials. *Biosci Rep*. 2019;39:BSR20180992. doi:10.1042/BSR20180992
6. Choi C, Benveniste EN. Fas ligand/Fas system in the brain: regulator of immune and apoptotic responses. *Brain Res Rev*. 2004;44:65–81. doi:10.1016/j.brainresrev.2003.08.007

7. Volpe E, Sambucci M, Battistini L, Borsellino G. Fas–Fas ligand: checkpoint of T cell functions in multiple sclerosis. *Front Immunol*. 2016;7:382. doi:10.3389/fimmu.2016.00382
8. Yamada A, Arakaki R, Saito M, Kudo Y, Ishimaru N. Dual role of Fas/FasL-mediated signal in peripheral immune tolerance. *Front Immunol*. 2017;8:403. doi:10.3389/fimmu.2017.00403
9. Mikoś H, Mikoś M, Obara-Moszyńska M, Niedziela M. The role of the immune system and cytokines involved in the pathogenesis of autoimmune thyroid disease (AITD). *Endokrynol Pol*. 2014;65:150–155. doi:10.5603/EP.2014.0021
10. Stassi G, De Maria R. Autoimmune thyroid disease: new models of cell death in autoimmunity. *Nat Rev Immunol*. 2002;2:195–204. doi:10.1038/nri750
11. Mahdi R, Al Jothery A, Msayer K, Al-Hassnawi A. Effect of thyroid dysfunction on apoptosis markers: caspase-3 and Bcl-2 among Iraqi patients. *Egypt J Immunol*. 2025;32:50–55. doi:10.55133/eji.320105
12. Gao Y, Luan X, Melamed J, Brockhausen I. Role of glycans on key cell surface receptors that regulate cell proliferation and cell death. *Cells*. 2021;10:1252. doi:10.3390/cells10051252
13. Reily C, Stewart TJ, Renfrow MB, Novak J. Glycosylation in health and disease. *Nat Rev Nephrol*. 2019;15:346–366. doi:10.1038/s41581-019-0129-4
14. Trzos S, Link-Lenczowski P, Pocheć E. The role of N-glycosylation in B-cell biology and IgG activity. The aspects of autoimmunity and anti-inflammatory therapy. *Front Immunol*. 2023;14:1188838. doi:10.3389/fimmu.2023.1188838
15. Munkley J, Elliott DJ. Hallmarks of glycosylation in cancer. *Oncotarget*. 2016;7:35478–35489. doi:10.18632/oncotarget.8155
16. Seyrek K, Richter M, Lavrik IN. Decoding the sweet regulation of apoptosis: the role of glycosylation and galectins in apoptotic signaling pathways. *Cell Death Differ*. 2019;26:981–993. doi:10.1038/s41418-019-0317-6
17. Peixoto A, Relvas-Santos M, Azevedo R, Santos LL, Ferreira JA. Protein glycosylation and tumor microenvironment alterations driving cancer hallmarks. *Front Oncol*. 2019;9:380. doi:10.3389/fonc.2019.00380
18. Swindall AF, Bellis SL. Sialylation of the Fas death receptor by ST6Gal-I provides protection against Fas-mediated apoptosis in colon carcinoma cells. *J Biol Chem*. 2011;286:22982–22990. doi:10.1074/jbc.M110.211375
19. Jan M, Upadhyay C, Alcami Pertejo J, Hioe CE, Arora SK. Heterogeneity in glycan composition on the surface of HIV-1 envelope determines virus sensitivity to lectins. *PLoS One*. 2018;13:e0194498. doi:10.1371/journal.pone.0194498
20. Li Z, Huang Y, Dong F, et al. Swainsonine promotes apoptosis in human oesophageal squamous cell carcinoma cells in vitro and in vivo through activation of mitochondrial pathway. *J Biosci*. 2012;37:1005–1016. doi:10.1007/s12038-012-9265-8
21. Hanly EK, Rajoria S, Darzynkiewicz Z, et al. Disruption of mutated BRAF signaling modulates thyroid cancer phenotype. *BMC Res Notes*. 2014;7:187. doi:10.1186/1756-0500-7-187
22. Kopp S, Warnke E, Wehland M, et al. Mechanisms of three-dimensional growth of thyroid cells during long-term simulated microgravity. *Sci Rep*. 2015;5:16691. doi:10.1038/srep16691
23. Ząbczyńska M, Polak K, Kozłowska K, Sokołowski G, Pocheć E. The contribution of IgG Glycosylation to Antibody-Dependent Cell-Mediated Cytotoxicity (ADCC) and Complement-Dependent Cytotoxicity (CDC) in Hashimoto's thyroiditis: an in vitro model of thyroid autoimmunity. *Biomolecules*. 2020;10:171. doi:10.3390/biom10020171
24. Wang S, Liu Y, Zhao N, et al. IL-34 expression is reduced in Hashimoto's thyroiditis and associated with thyrocyte apoptosis. *Front Endocrinol*. 2018;9:629. doi:10.3389/fendo.2018.00629
25. Cui L, Liu S, Ding Y, et al. IL-1beta sensitizes rat intervertebral disc cells to Fas ligand mediated apoptosis in vitro. *Acta Pharmacol Sin*. 2007;28:1671–1676. doi:10.1111/j.1745-7254.2007.00642.x
26. Ząbczyńska M, Link-Lenczowski P, Novokmet M, et al. Altered N-glycan profile of IgG-depleted serum proteins in Hashimoto's thyroiditis. *Biochim Biophys Acta - Gen Subj*. 2020;1864:129464. doi:10.1016/j.bbagen.2019.129464
27. Link-Lenczowski P, Bubka M, Balog CIA, et al. The glycomic effect of N-acetylglucosaminyltransferase III overexpression in metastatic melanoma cells. GnT-III modifies highly branched N-glycans. *Glycoconjugate J*. 2018;35:217–231. doi:10.1007/s10719-018-9814-y
28. Packer NH, Lawson MA, Jardine DR, Redmond JW. A general approach to desalting oligosaccharides released from glycoproteins. *Glycoconjugate J*. 1998;15:737–747. doi:10.1023/A:1006983125913
29. Reiding KR, Blank D, Kuijper DM, Deelder AM, Wuhrer M. High-throughput profiling of protein N-Glycosylation by MALDI-TOF-MS employing linkage-specific sialic acid esterification. *Anal Chem*. 2014;86:5784–5793. doi:10.1021/ac500335t
30. Opydo-Chanek M, Cichoń I, Rak A, Kołaczkowska E, Mazur L. The pan-Bcl-2 inhibitor obatoclax promotes differentiation and apoptosis of acute myeloid leukemia cells. *Invest New Drugs*. 2020;38:1664–1676. doi:10.1007/s10637-020-00931-4
31. Keppler OT, Peter ME, Hinderlich S, et al. Differential sialylation of cell surface glycoconjugates in a human B lymphoma cell line regulates susceptibility for CD95 (APO-1/Fas)-mediated apoptosis and for infection by a lymphotropic virus. *Glycobiology*. 1999;9:557–569. doi:10.1093/glycob/9.6.557
32. Lavine CL, Lao S, Montefiori DC, Haynes BF, Sodroski JG, Yang X. High-Mannose glycan-dependent epitopes are frequently targeted in broad neutralizing antibody responses during human immunodeficiency virus type 1 infection. *J Virol*. 2012;86:2153–2164. doi:10.1128/JVI.06201-11
33. Wang S, Guo Y, Yang C, et al. Swainsonine triggers paraptosis via ER stress and MAPK signaling pathway in rat primary renal tubular epithelial cells. *Front Pharmacol*. 2021;12:715285. doi:10.3389/fphar.2021.715285
34. Varki A, Cummings RD, Aebi M, et al. Symbol nomenclature for graphical representations of glycans. *Glycobiology*. 2015;25:1323–1324. doi:10.1093/glycob/cwv091
35. Bossowski A, Czarnocka B, Bardadin K, et al. Identification of apoptotic proteins in thyroid gland from patients with Graves' disease and Hashimoto's thyroiditis. *Autoimmunity*. 2008;41:163–173. doi:10.1080/08916930701727749
36. Li Z, Wang J, Tang C, Wang X, Zou S. Regulative effect of IFN-gamma on the Fas/Fas L system of cholangiocarcinoma cells. *Zhonghua Yu Fang Yi Xue Za Zhi*. 2002;36:495–498.
37. Li Z, Xu X, Huang Y, et al. Swainsonine activates mitochondria-mediated apoptotic pathway in human lung cancer A549 cells and retards the growth of lung cancer xenografts. *Int J Biol Sci*. 2012;8:394–405. doi:10.7150/ijbs.3882
38. Lichtenstein RG, Rabinovich GA. Glycobiology of cell death: when glycans and lectins govern cell fate. *Cell Death Differ*. 2013;20:976–986. doi:10.1038/cdd.2013.50

39. Shatnyeva OM, Kubarenko AV, Weber CEM, et al. Modulation of the CD95-induced apoptosis: the role of CD95 N-glycosylation. *PLoS One*. 2011;6:e19927. doi:10.1371/journal.pone.0019927
40. Mezosi E, Wang SH, Utsugi S, et al. Induction and regulation of Fas-mediated apoptosis in human thyroid epithelial cells. *Mol Endocrinol*. 2005;19:804–811. doi:10.1210/me.2004-0286
41. Radovani B, Gudelj I. N-Glycosylation and Inflammation; the not-so-sweet relation. *Front Immunol*. 2022;13:893365. doi:10.3389/fimmu.2022.893365
42. Kawakami A, Euguchi K, Matsuoka N, et al. Modulation of Fas-mediated apoptosis of human thyroid epithelial cells by IgG from patients with Graves' disease (GD) and idiopathic myxoedema. *Clin Exp Immunol*. 2003;110:434–439. doi:10.1046/j.1365-2249.1997.4301447.x
43. Holdbrooks A, Schultz MJ, Liu Z, Bullard D, Bellis SL. Abstract 3566: glycosylation of the TNFR1 death receptor controls cell fate. *Cancer Res*. 2016;76:3566. doi:10.1158/1538-7445.AM2016-3566
44. Lv H, Zhang S, Hao X. Expression of Concern: swainsonine protects H9c2 cells against lipopolysaccharide-induced apoptosis and inflammatory injury via down-regulating miR-429. *Cell Cycle*. 2021;20:2669. doi:10.1080/15384101.2021.1973194
45. Gottlieb E, Armour SM, Harris MH, Thompson CB. Mitochondrial membrane potential regulates matrix configuration and cytochrome c release during apoptosis. *Cell Death Differ*. 2003;10:709–717. doi:10.1038/sj.cdd.4401231
46. Colley K, Varki A, Haltiwanger R, et al. Cellular Organization of Glycosylation. In: Varki A, Cummings R, Esko J, et al. editors. *Essentials of Glycobiology*. NY: Cold Spring Harbor Laboratory Press; 2022. doi:10.1101/glycobiology.4e.4
47. Ohtsubo K, Marth JD. Glycosylation in cellular mechanisms of health and disease. *Cell*. 2006;126:855–867. doi:10.1016/j.cell.2006.08.019